RSC Advances

PAPER

View Article Online
View Journal | View Issue

Cite this: *RSC Adv.*, 2017, **7**, 30984

Mechanistic investigation on radical-induced construction of oxindoles: radical *versus* electrophilic cyclization†

Zhiqiang Deng,[a] Lu Jin,[ab] Yong Wu *[a] and Xiang Zhao *[a]

Received 27th April 2017
Accepted 8th June 2017

DOI: 10.1039/c7ra04756h

rsc.li/rsc-advances

This work is based on our previous reported experimental results (*RSC Advances*, 2016, **6**, 27000). The mechanism of constructing oxindoles *via* tandem radical reaction of *N*-arylacrylamide with tertiary cycloalkanols is theoretically explored by using density functional theory (DFT). A four-step mechanism was put forward for the reaction. Step 1 is related with the ring-opening process of cycloalkanol radical after the oxidation, step 2 corresponds to the intermolecular attack between keto-included alkyl radical and *N*-methyl-*N*-phenylmethacrylamide, step 3 is associated with the intramolecular C–C bond formation *via* the cationic attack, and step 4 is the deprotonation towards the final product. It is found that step 2 is the rate-limiting step. Importantly, step 3 is updated to be a cationic step (channel 2), instead of the previously suggested radical step (channel 1). After the ring-opening processes, comparative study indicates that the intramolecular reactions of β-, γ-, and δ-keto radicals determines the product selectivity. The low selectivity of product in the cyclopentanol-involved reaction would originate from the high competition between intra- and intermolecular reactions, which is in agreement with our previous experimental observations.

1. Introduction

Tandem reactions, which combine multiple reaction steps into a single operation, are powerful and extensively used in organic synthesis.[1–4] Due to the advantage of atom and step economy, this strategy has been focused by synthetic chemists and was comprehensively applied in total synthesis.[5–9] In recent years, thanks to tandem radical cyclization strategy, the easily accessible *N*-arylacrylamides have been widely used for the synthesis of 3,3-disubstituted oxindole skeletons[10–13] which commonly exist in numerous natural compounds.[14–16] It is easy to put a variety of functional groups on the C3-position of oxindoles with different radical substrates.

Based on the research interest in the synthesis of oxindoles derivatives,[17–21] we have systematically studied a novel transition-metal free tandem radical cyclization of acrylamides with tertiary cycloalkanol.[22] To our delight, we achieved the first combination of ring-opening of tertiary cycloalkanols and functionalization of acrylamides *via* the tandem radical cyclization reaction (Scheme 1a). To gain insight into the mechanism of this reaction, we have also tested two radical scavengers (TEMPO and BHT) under the optimal reaction condition to trap the forming radical in the reaction. In addition, the intra- and intermolecular kinetic isotope effect (KIE) experiments were also performed, respectively. According to the experimental results, we suggested that the reaction might undergo a radical pathway (Scheme 1b).

Although this mechanism could be accepted widely,[23–34] some critical issues deserve to take into account. In particular, several details of the reaction mechanism need to be clarified. For example, how to understand the competition between intramolecular cyclization and intermolecular addition? Which step determines the rate of the reaction? And how much is about the redox potential for each reactive intermediates? Generally, it is tough to thoroughly observe and respond these points using experimental methods only. On the other hand, quantum mechanics (QM) computations can practically find the trajectory of reaction processes and provide electronic structure information in detail.

In this work, the reaction mechanism of the experimental reaction (Scheme 1a) is examined by using density functional theory (DFT) method at the M06-2X/6-31+G(d,p) level. Our computations reveal that a four-step mechanism is involved in the radical-induced construction of oxindoles and that the intermolecular attack of cycloalkanol radical on the double bond of acrylamide (II → III, Scheme 1b) is the rate-determining step. Interestingly, except the conventional

[a]*Department of Chemistry, Institute for Chemical Physics, School of Science, Xi'an Jiaotong University, Xi'an 710049, China. E-mail: xzhao@mail.xjtu.edu.cn; specwy@mail.xjtu.edu.cn*

[b]*College of Chemical Engineering, Xinjiang Agriculture University, Urumchi, 830025, China*

† Electronic supplementary information (ESI) available: Computational details of reduction potential, calculated energies, Cartesian coordinates of stationary points, and relative energy profiles for comparative studies. See DOI: 10.1039/c7ra04756h

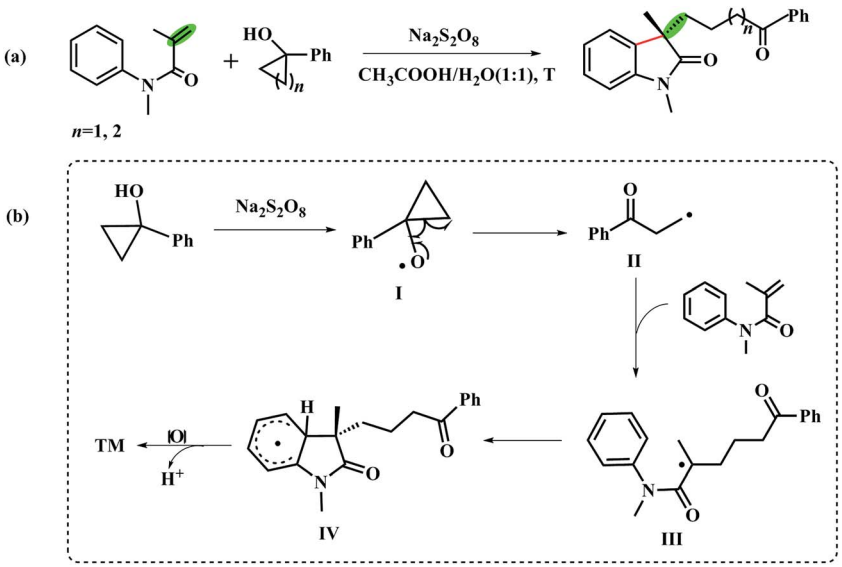

Scheme 1 (a) Transition-metal free catalyzed cyclization reaction of acrylamides with the tertiary cycloalkanols. (b) The proposed reaction mechanism in ref. 22.

radical intramolecular ring closure (III → IV, Scheme 1b), we put forward a intramolecular electrophilic ring closure for the formation of oxindole *via* a cationic step after the oxidization. The evidence of the calculated redox potential supports this cationic step is favorable in the reaction. To the best of our knowledge, it is the first time to demonstrate the favored intramolecular electrophilic cyclization in the radical-induced construction of oxindole.

2. Computational details

All relevant structures were fully optimized at the M06-2X/6-31+G(d,p) level, combined with self-consistent reaction field (SCRF) method. Frequency analysis was used to ensure each optimized stationary point to be a minimum or a saddle point. Intrinsic reaction coordinate (IRC) calculations were also performed to verify that each transition state connects with the two associated minima on the potential energy surface. The solvent effect was evaluated in water ($\varepsilon = 78.4$) with the conductor-like polarized continuum model (C-PCM). To match with the experimental conditions, all thermal energies were corrected at 50 °C and 1 atm. Furthermore, some electronic structures were analyzed by the natural bond orbital (NBO) method. All computations were performed with Gaussian 09 package.[35] All 3-D structures were generated by CYLview program.[36]

3. Results and discussion

3.1. 1-Phenylcyclopropanol-related reaction mechanism

In this study, 1-phenylcyclopropanol and *N*-methyl-*N*-phenylmethacrylamide as the substrates were selected to explore the reaction mechanism. According to our computational results, we divide the overall reaction into four steps to report in this article. Step 1 is related with the ring-opening of 1-phenylcyclopropanol radical after the oxidation, step 2 is corresponding to the intermolecular attack between β-keto radical and *N*-methyl-*N*-phenylmethacrylamide, step 3 is associated with intramolecular ring closure to construct a C–C bond, and step 4 is the deprotonation towards the final product.

3.1.1. Ring-opening of 1-phenylcyclopropanol radical (step 1). At first, we deem that 1-phenylcyclopropanol would be easy to form a radical under the external oxidant $Na_2S_2O_8$ *via* a proton-coupling electron transfer (PCET) process. As illustrated in Fig. 1, we optimized the radical **A-INT-Ra1**. The corresponding bond length of C1–C2 (or C1–C3) is 1.606 Å, which is about 0.160 Å longer than that of C2–C3. The spin density reveals that, except the non-bonding orbital of O1, the unpaired electron is partially delocalized in C1–C2 and C1–C3 σ bonds. The natural bond orbital (NBO) analysis also indicates that the electron would transfer from the non-bonding orbital n(O) to the σ*(C1–C2) and σ*(C1–C3) orbitals, meanwhile the electron would transfer back from σ(C1–C2) and σ(C1–C3) orbitals to unpaired n(O) orbital. In this way, C1–C2 and C1–C3 bonds are weaken to facilitate the ring-opening *via* the C–C bond cleavage. Obviously, it is equivalent for breaking C1–C2 and C1–C3 bonds in this system. Therefore, C1–C2 bond cleavage was considered in the paragraph for an unified statement. The related transition state **A-TS-Ra1** was optimized on the potential energy surface (Fig. 2). In **A-TS-Ra1**, the distance of C1–C2 increases to 1.830 Å, whereas the distance of C1–C3 decreases to 1.542 Å. Vibrational analysis indicates that the imaginary frequency is almost related with the C1–C2 bond stretch mode. Then the reaction offers a β-keto radical **A-INT-Ra2**. The spin density indicates that the unpaired electron is mainly localized on the C2 atom. As also shown in Fig. 2, one can see that the $\Delta G^{\ddagger}$ is very low (*ca.* 0.8 kcal mol^{-1}) from **A-INT-Ra1** to **A-TS-Ra1** and that the Gibbs free energy dramatically drops down, indicating that this ring-opening process is very easy to take place and strongly irreversible.

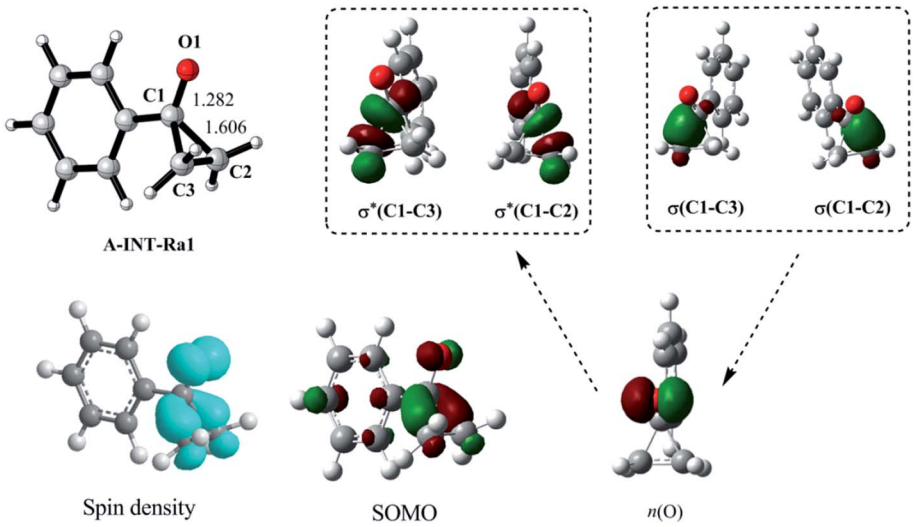

Fig. 1 Geometry, spin density, single occupied molecular orbital (SOMO), and correlations of natural orbitals, for the radical **A-INT-Ra1**. n(O) is an unpaired p orbital.

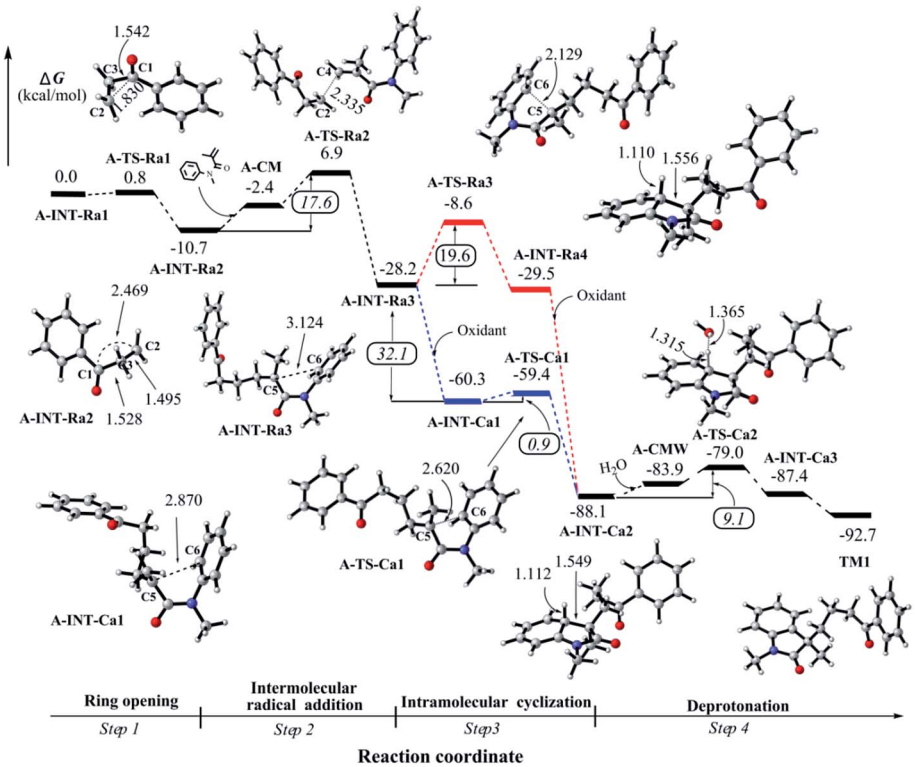

Fig. 2 Relative Gibbs free energy profiles for the title reaction. Radical (channel 1, upper) and electrophilic (channel 2, below) cyclizations in step 3 are labeled as red and blue lines, respectively.

3.1.2. Intermolecular radical addition between β-keto radical and *N*-methyl-*N*-phenylmethacrylamide (step 2). After the formation of the radical **A-INT-Ra2**, there would be two pathways to undergo. Pathway 1 is the intermolecular attack on the C=C double bond of *N*-methyl-*N*-phenylmethacrylamide; pathway 2 is to construct a five-membered ring by the intramolecular attack on the vicinal aromatic ring. As shown in the ESI† and discussed in the next section, we found that pathway 2 would be unlikely to undergo in this step of the reaction. Herein we firstly report the favored intermolecular attack process.

After the formation of a loose complex **A-CM** between **A-INT-Ra2** and *N*-methyl-*N*-phenylmethacrylamide, the corresponding transition state **A-TS-Ra2** was optimized (see Fig. 2). The distribution of spin density indicates that the unpaired electron

partially moves to *N*-methyl-*N*-phenylmethacrylamide in **A-TS-Ra2** (see Fig. S4 in the ESI†). The bond distance of C2–C4 is 2.335 Å. The $\Delta G^{\ddagger}$ is 17.6 kcal mol^{-1} in this step. Then the C2–C4 single bond is formed in the intermediate **A-INT-Ra3**. It is found that this intermolecular attack step is a strongly irreversible process where the Gibb free energy drops down 17.5 kcal mol^{-1} from **A-INT-Ra2**. In **A-INT-Ra3**, the spin density is expectedly localized on C5 atom. The unpaired electron would be stabilized by the π-conjugation of amide moiety.

3.1.3. Intramolecular ring closure to construct a C–C bond (step 3). Next, we firstly conventionally considered the intramolecular radical cyclization (channel 1). As also shown in Fig. 2, the transition state **A-TS-Ra3** was obtained. The corresponding C5–C6 bond distance is 2.129 Å. However, the $\Delta G^{\ddagger}$ is 19.6 kcal mol^{-1}, which indicates that the lifetime of **A-INT-Ra3** would be somewhat long. In this sense, whether the radical intermediate **A-INT-Ra3** could be oxidized to a cation or not in the presence of the external oxidant.

Alternatively, the intramolecular electrophilic cyclization (channel 2), namely Friedel–Crafts reaction, was taken into account in this work. We tested the possibility for the oxidation of **A-INT-Ra3** by using the external oxidant $Na_2S_2O_8$. The computational details for the redox potential is provided in the ESI.† Our results indicate that the redox potential is about −32.1 kcal mol^{-1} (−1.39 eV),[37,38] revealing that it would be likely to promote the radical to a cation in the presence of external oxidant $Na_2S_2O_8$. The high potential and irreversibility would partially benefit from the conjugation effect of the amide moiety. Interestingly, we found that the electrophilic cyclization is very easy to undergo with a barrier of 0.9 kcal mol^{-1} (Fig. 2). After checking the structural parameters, we found that the transition state **A-TS-Ca1** is very close to **A-INT-Ca1**. The bond distance of C5–C6 is 2.620 in **A-TS-Ca1**, whereas it is 2.870 Å in **A-INT-Ca1**. The imaginary vibrational frequency, which is associated with C5–C6 bond stretch mode, is only 73.8 cm^{-1}. Both the reactant-like structure and low imaginary vibrational frequency support this electrophilic cyclization would be a low energy barrier step. That is to say, once the radical **A-INT-Ra3** is oxidized to the cation **A-INT-Ca1**, the process of cyclization would be much easier to take place. After the C–C bond formation, another cation **A-INT-Ca2** is offered in the reaction. The corresponding Gibbs free energy continues dramatically dropping down by about 30.0 kcal mol^{-1}.

3.1.4. Deprotonation towards the final product (step 4). Finally, with the requirement of the aromatization, the cation intermediate **A-INT-Ca2** would undergo deprotonation to furnish the final product **TM1**. Obviously, this step would be rapid with the help of water or an anion. Therefore, we roughly estimated the Gibbs free energy barrier for this deprotonation by adding one explicit water to abstract this proton. Computational results show that it only needs about 9.1 kcal mol^{-1} for the deprotonation with one explicit water. If using an anion, such as SO_4^{2-}, to abstract this proton, it would be undoubtedly more favorable.

In all, the mechanistic scenario of the tandem reaction is clarified for 1-phenylcyclopropanol and *N*-methyl-*N*-phenylmethacrylamide by using DFT method. The reaction would be triggered by a proton-coupling electron transfer (PCET) process in the presence of the external oxidant, leading to a radical whose spin density is not only localized on the oxygen atom but also distributes in C–C bonds. Next, it would be very easy to undergo the ring-opening of 1-phenylcyclopropanol to afford a β-keto radical whose spin density is mainly localized on the distal carbon atom. After that, the addition of the β-keto radical to the double bond of *N*-methyl-*N*-phenylmethacrylamide would happen. Then the intramolecular cyclization would undergo an unexpected cationic process after the oxidation of the formed radical intermediate. Finally, the deprotonation would easily

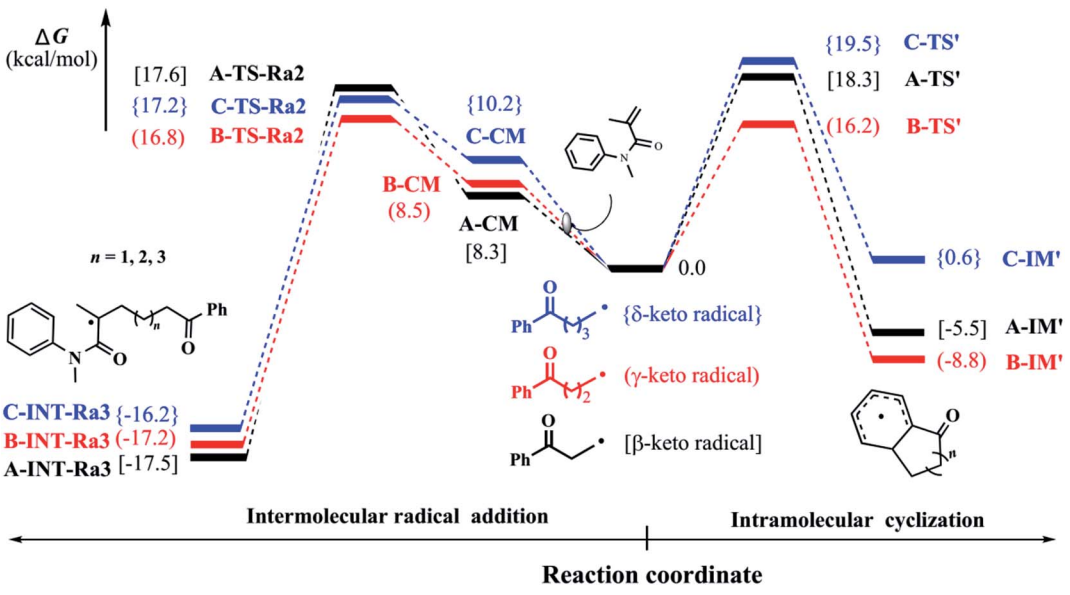

Fig. 3 Relative Gibbs free energy (kcal mol^{-1}) profiles of β-, γ-, δ-keto radicals for intramolecular radical cyclization and intermolecular radical addition.

occur to generate the product. Our results indicate that step 2 is the rate-limiting step in the overall reaction, which is consistent with the experimental KIE observations.

3.2. Comparative study on the reactions of tertiary cyclobutanol or cyclopentanol with *N*-arylacrylamides

Based on the results as mentioned above, we also expand our scope on the reactions of tertiary cyclobutanol or cyclopentanol with *N*-arylacrylamides. The detailed results are shown in the ESI.† As we expected, the large different exists in the ring-opening step of the cyclobutanol or cyclopentanol radicals after the oxidation (step 1). Due to the smaller ring strain in cyclobutanol and cyclopentanol radicals, the corresponding $\Delta G^{\ddagger}$ of ring-opening slightly increases to 1.2 and 6.2 kcal mol^{-1}, respectively. As for other reaction processes, we found that the trend are very similar to the aforementioned mechanism and that the intramolecular electrophilic cyclization would also be more favorable *via* the cationic process in step 3.

3.3. Intramolecular dearomatization after the ring-opening of cycloalcohol radicals

In our previous experiments, the benzocyclohexanone, an intramolecular addition byproduct, was always detected. Therefore, we attempted to make clear this phenomenon in our study. Starting from keto-included alkyl radicals which generate from the ring-opening of the corresponding cycloalcohol radicals, we explored the intramolecular dearomatization processes (denoted as pathway 2 as mentioned above). Fig. 3 shows the corresponding Gibbs free energy barriers of the intramolecular radical cyclizations in the keto-included alkyl radicals (β-, γ-, and δ-keto radicals). Due to the little ring constrain, the ring-closure $\Delta G^{\ddagger}$ of γ-keto radical would be the lowest *via* a six-remembered cyclic transition state. Compared with the intermolecular radical addition as stated above, the barriers ($\Delta G^{\ddagger}$) of intramolecular ring-closure processes for β- and δ-keto radicals are somewhat higher. It is very important to note that the $\Delta G^{\ddagger}$ of γ-keto radical in the intramolecular ring-closure is slightly lower than that of intermolecular radical addition process. Therefore, the low selectivity of product in the cyclopentanol-involved reaction would originate from the high competition between intra- and intermolecular reactions, which is in agreement with our experimental observations.

4. Conclusions

The mechanism of constructing oxindoles *via* tandem radical reaction of *N*-arylacrylamide with tertiary cycloalkanols was theoretically explored by using density functional theory (DFT) method in this work. Our findings are summarized as follows.

(1) A four-step mechanism was put forward for the title reaction. Step 1 is related with the ring-opening process of 1-phenylcyclopropanol radical after the oxidation, step 2 is corresponding to the intermolecular attack between β-keto radical and *N*-methyl-*N*-phenylmethacrylamide, step 3 is associated with the intramolecular C–C bond formation *via* the cationic attack, and step 4 is the deprotonation towards the final product.

(2) Step 2, an intermolecular radical attack, is the rate-limiting step in the overall reaction.

(3) Step 3 was updated to a novel cationic intramolecular ring closure, which is different from the radical process in our previous suggestion.

(4) After the ring-opening processes, comparative study indicates that the intramolecular reactions of β-, γ-, and δ-keto radicals determine the product selectivity. The low selectivity of product in the cyclopentanol-involved reaction would originate from the high competition between intra- and intermolecular reactions.

This novel mechanism of the unexpected cationic intramolecular ring closure enriches the understanding of constructing oxindoles and provides the possibility to control the reaction selectivity. Moreover, it is very crucial for other similar radical reaction to draw a rational mechanism.

Acknowledgements

This work was supported by the National Natural Science Foundation of China (No. 21573172) and the National Key Basic Research Program of China (No. 2012CB720904). L. Jin thanks the Postdoctoral Science Foundation of China (No. 2015M582635) and Research Foundation for Advanced Talents in Xinjiang Province. Y. Wu thanks the Fundamental Research Funds for the Central University (No. xjj2015064).

References

1 S. E. Denmark and A. Thorarensen, *Chem. Rev.*, 1996, **96**, 137–165.
2 J. H. Kim, Y. O. Ko, J. Bouffard and S. Lee, *Chem. Soc. Rev.*, 2015, **44**, 2489–2507.
3 L. F. Tietze, *Chem. Rev.*, 1996, **96**, 115–136.
4 L. F. Tietze and U. Beifuss, *Angew. Chem., Int. Ed.*, 1993, **32**, 131–163.
5 R. A. Bunce, *Tetrahedron*, 1995, **51**, 13103–13159.
6 K. C. Nicolaou, D. J. Edmonds and P. G. Bulger, *Angew. Chem., Int. Ed.*, 2006, **45**, 7134–7186.
7 K. C. Nicolaou, Q. Kang, T. R. Wu, C. S. Lim and D. Y. K. Chen, *J. Am. Chem. Soc.*, 2010, **132**, 7540–7548.
8 K. C. Nicolaou and J. Li, *Angew. Chem., Int. Ed.*, 2001, **40**, 4264–4268.
9 K. C. Nicolaou, T. Montagnon and S. A. Snyder, *Chem. Commun.*, 2003, 551–564.
10 J. Bergman, *Advances in Heterocyclic Chemistry*, ed. E. F. V. Scriven and C. A. Ramsden, Elsevier Academic Press Inc, San Diego, 2015, vol. 117, pp. 1–81.
11 J. R. Chen, X.-Y. Yu and W.-J. Xiao, *Synthesis*, 2015, **47**, 604–629.
12 C. C. Li and S. D. Yang, *Org. Biomol. Chem.*, 2016, **14**, 4365–4377.
13 R. J. Song, Y. Liu, Y. X. Xie and J. H. Li, *Synthesis*, 2015, **47**, 1195–1209.

14 N. R. Ball-Jones, J. J. Badillo and A. K. Franz, *Org. Biomol. Chem.*, 2012, **10**, 5165–5181.
15 C. V. Galliford and K. A. Scheidt, *Angew. Chem., Int. Ed.*, 2007, **46**, 8748–8758.
16 H. Lin and S. J. Danishefsky, *Angew. Chem., Int. Ed.*, 2003, **42**, 36–51.
17 Y. Meng, L. N. Guo, H. Wang and X.-H. Duan, *Chem. Commun.*, 2013, **49**, 7540–7542.
18 H. Wang, L. N. Guo and X.-H. Duan, *Chem. Commun.*, 2013, **49**, 10370–10372.
19 H. Wang, L. N. Guo and X.-H. Duan, *Adv. Synth. Catal.*, 2013, **355**, 2222–2226.
20 H. Wang, L. N. Guo and X.-H. Duan, *J. Org. Chem.*, 2016, **81**, 860–867.
21 S. L. Zhou, L. N. Guo, H. Wang and X.-H. Duan, *Chem.–Eur. J.*, 2013, **19**, 12970–12973.
22 L. N. Guo, Z. Q. Deng, Y. Wu and J. Hu, *RSC Adv.*, 2016, **6**, 27000–27003.
23 W. Fu, F. Xu, Y. Fu, M. Zhu, J. Yu, C. Xu and D. Zou, *J. Org. Chem.*, 2013, **78**, 12202–12206.
24 W. J. Fu, F. J. Xu, Y. Q. Fu, M. Zhu, J. Q. Yu, C. Xu and D. P. Zou, *J. Org. Chem.*, 2013, **78**, 12202–12206.
25 Y. M. Li, Y. H. Shen, K. J. Chang and S. D. Yang, *Tetrahedron*, 2014, **70**, 1991–1996.
26 Y. M. Li, X. H. Wei, X. A. Li and S. D. Yang, *Chem. Commun.*, 2013, **49**, 11701–11703.
27 Z. Li, Y. Zhang, L. Zhang and Z. Q. Liu, *Org. Lett.*, 2014, **16**, 382–385.
28 M. Z. Lu and T. P. Loh, *Org. Lett.*, 2014, **16**, 4698–4701.
29 X. H. Ouyang, R. J. Song and J. H. Li, *Eur. J. Org. Chem.*, 2014, **2014**, 3395–3401.
30 T. Shen, Y. Yuan, S. Song and N. Jiao, *Chem. Commun.*, 2014, **50**, 4115–4118.
31 X. J. Tang, C. S. Thomoson and W. R. Dolbier, *Org. Lett.*, 2014, **16**, 4594–4597.
32 J. Y. Wang, X. Zhang, Y. Bao, Y. M. Xu, X. F. Cheng and X.-S. Wang, *Org. Biomol. Chem.*, 2014, **12**, 5582–5585.
33 W. T. Wei, M. B. Zhou, J. H. Fan, W. Liu, R. J. Song, Y. Liu, M. Hu, P. Xie and J. H. Li, *Angew. Chem., Int. Ed.*, 2013, **52**, 3638–3641.
34 P. Xu, J. Xie, Q. C. Xue, C. D. Pan, Y. X. Cheng and C. J. Zhu, *Chem.–Eur. J.*, 2013, **19**, 14039–14042.
35 M. J. Frisch, G. W. Trucks, H. B. Schlegel, G. E. Scuseria, M. A. Robb, J. R. Cheeseman, G. Scalmani, V. Barone, B. Mennucci, G. A. Petersson, H. Nakatsuji, M. Caricato, X. Li, H. P. Hratchian, A. F. Izmaylov, J. Bloino, G. Zheng, J. L. Sonnenberg, M. Hada, M. Ehara, K. Toyota, R. Fukuda, J. Hasegawa, M. Ishida, T. Nakajima, Y. Honda, O. Kitao, H. Nakai, T. Vreven, J. A. Montgomery Jr, J. E. Peralta, F. Ogliaro, M. Bearpark, J. J. Heyd, E. Brothers, K. N. Kudin, V. N. Staroverov, R. Kobayashi, J. Normand, K. Raghavachari, A. Rendell, J. C. Burant, S. S. Iyengar, J. Tomasi, M. Cossi, N. Rega, J. M. Millam, M. Klene, J. E. Knox, J. B. Cross, V. Bakken, C. Adamo, J. Jaramillo, R. Gomperts, R. E. Stratmann, O. Yazyev, A. J. Austin, R. Cammi, C. Pomelli, J. W. Ochterski, R. L. Martin, K. Morokuma, V. G. Zakrzewski, G. A. Voth, P. Salvador, J. J. Dannenberg, S. Dapprich, A. D. Daniels, Ö. Farkas, J. B. Foresman, J. V. Ortiz, J. Cioslowski and D. J. Fox, *Gaussian 09*, Gaussian, Inc., Wallingford CT, 2009.
36 C. Y. Legault, *CYLView, 1.0b*, Université de Sherbrooke, Canada, 2009, http://www.cylview.org.
37 W. S. Chen, Y. C. Jhou and C. P. Huang, *Chem. Eng. J.*, 2014, **252**, 166–172.
38 C. Liang and H. W. Su, *Ind. Eng. Chem. Res.*, 2009, **48**, 5558–5562.